

Factors Affecting the Infrared and Raman Spectra of Rutile Powders

M. OCAÑA AND V. FORNÉS

Instituto de Ciencia de Materiales, CSIC, Serrano 115 bis, 28006 Madrid, Spain

J. V. GARCÍA RAMOS

Instituto de Optica, CSIC, Serrano 121, 28006 Madrid, Spain

AND C. J. SERNA

Instituto de Ciencia de Materiales, CSIC, Serrano 115 bis, 28006 Madrid, Spain

Received October 16, 1987

The utility of infrared and Raman spectroscopy in the characterization of powdered samples is illustrated for the case of TiO_2 (rutile). Particle shape and state of aggregation of the microcrystals are shown to have a strong effect on the infrared powder spectra as predicted by the Theory of the Average Dielectric Constant. On the other hand, surface effects related to particle size can be observed in the Raman spectra by the appearance of new bands as the surface to volume ratio increases. Finally, it is shown that the nonstoichiometric character of rutile does not have a significant effect in the infrared powder spectra. © 1988 Academic Press, Inc.

Introduction

Theoretical considerations show that the vibrational spectra, infrared and Raman, of a powdered sample contains information not only on the phases present but also on the size, shape, and state of aggregation of the microcrystals that constitute the powder (1-4). The position, relative intensity, and width of the infrared or Raman bands can be, in principle, affected by the above effects due to the polarization charge induced on the particle surface by the external electromagnetic field. Experimental observations of these effects have been reported for the infrared spectra of several

microcrystalline solids (2, 4-8) and to a lesser extent also for the Raman spectrum (9-12). Thus, vibrational spectroscopy could play an important role in the characterization of powders which is becoming very important since modern technology demands powders with chemical, structural, and morphological characteristics well defined.

The aim of the present work is to determine the contribution of different factors, i.e., size, shape, and state of aggregation of the microcrystals on the vibrational characteristics of TiO_2 (rutile) samples using the Theory of Average Dielectric Constant (TADC) which has been shown to give ac-

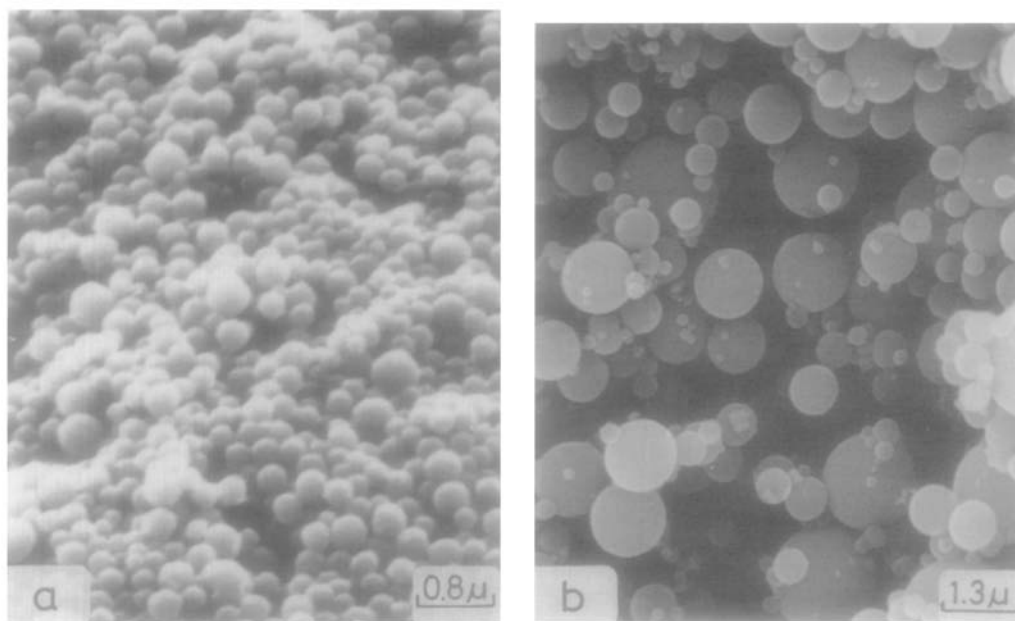


FIG. 1. SEM of TiO_2 (rutile) particles obtained by the aerosol technique: (a) constant N_2 flow rate (700 ml/min); (b) variable N_2 flow rate (500–800 ml/min).

curate results for powders with particle sizes smaller than the radiation wavelength (2, 13). In this theory, not only the shape of the particles are considered but also their state of aggregation since particle interactions are approximately incorporated in the theory.

Polarization effects can only be observed for vibrational modes which have translational character. Due to the centrosymmetric nature of rutile structure, such modes are active in the infrared but not in the Raman spectrum. Therefore, the effects of particle shape can be observed only in the infrared. Regarding the Raman spectrum, surface effects could be observed but only for very low particle sizes (11, 13).

In order to evaluate the effect of particle size and shape on the infrared absorption spectrum of microcrystalline rutile, monodispersed powders (uniform particle size and shape) obtained by different methods will be compared as well as during their evolution on sintering. Surface effects were

studied in the Raman spectra of very small rutile microcrystals ($\sim 400 \text{ \AA}$) obtained by hydrolysis of TiCl_4 .

It is well known that rutile is highly non-stoichiometric and variations in the stoichiometry may, in principle, affect the powder spectra. In this paper, the influence of non-stoichiometry on the powder spectra will also be studied in reduced samples with controlled morphology.

Experimental Procedure

Two types of monodispersed rutile powders were obtained using methods described in the literature (14, 15). The first one was prepared by hydrolysis of titanium ethoxide aerosol in an apparatus similar to that described by Visca and Matijevic (14). In all cases, the temperature of the falling film was kept at 90°C and AgCl heated to $\sim 700^\circ\text{C}$ was used as the nuclei generator. Monodispersed and polydispersed spherical powders (Figs. 1a and 1b) were obtained

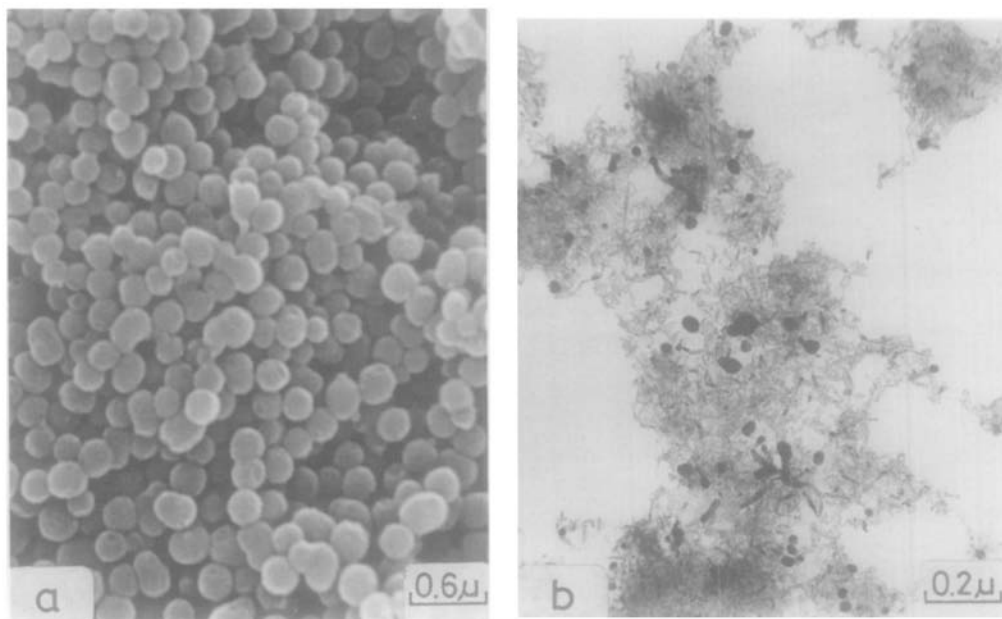


FIG. 2. (a) SEM of TiO_2 (rutile) particles obtained by hydrolysis of $\text{Ti}(\text{OC}_2\text{H}_5)_4$ in an alcoholic solution. (b) TEM of TiO_2 (rutile) particles obtained by hydrolysis of TiCl_4 at 98°C .

by altering the nitrogen flow rate. X-ray diffraction analysis of the TiO_2 particles collected after heating to 250°C showed the material to be essentially amorphous, but it can be transformed to rutile at $700\text{--}850^\circ\text{C}$, without sintering (Figs. 1a and 1b).

Monodispersed rutile powders were also obtained by hydrolysis of titanium ethoxide in ethanol solution at room temperature with a $\text{H}_2\text{O}/\text{alkoxide}$ molar ratio of 4.5 (15). The particles initially formed were amorphous to X-ray diffraction but they could be transformed to rutile after 10 hr of heating at 750°C (Fig. 2a). The particle size and shape of this powder was not as uniform as that obtained by the aerosol method and the electron microscope reveals spheres along with elongated particles. Similar results have been also observed by Jean and Ring (16).

In order to observe size effects in the Raman spectrum, rutile powders with very small particle size (modal diameter of about 400 \AA) were obtained by hydrolysis at 98°C

of a 3 M TiCl_4 solution. The sample was washed to remove chloride anions and dried at room temperature. The observation under the electron microscope clearly shows the polydispersed character of the sample (Fig. 2b).

Finally, nonstoichiometric rutile powders were obtained by reducing a high-temperature rutile sample under hydrogen atmosphere (10 Torr) at about 1200°C . On reduction the initially white powder started to darken becoming black at high reduction rates. Reoxidation of the reduced sample can be completely achieved at about 600°C under oxygen pressure.

All samples studied were rutile-type structure as determined by X-ray diffraction. The IR spectra were recorded in a Perkin-Elmer 580B spectrometer under such conditions yielding a resolution of better than 2 cm^{-1} . The sample dilution (KBr) was chosen so that the maximum absorption band would transmit no less than 20% of the incident energy. The infrared spectra

TABLE I
OPTICAL DATA OF TiO₂ RUTILE

Infrared				Raman	
Symmetry	ω_T	$4\pi\rho$	γ	Symmetry	ω
$A_{2u}(E C)$	172	165.00	0.440	B_{1g}	147
				a	235
	183	81.50	0.190	a	320–360
$E_u(E\perp C)$	388	1.08	0.058	E_g	446
	500	2.00	0.044	A_{1g}	610
				B_{2g}	826

Note. $\epsilon_z(//) = 8.4$; $\epsilon_z(\perp) = 6$.

^a Disorder or second-order scattering.

($K(\omega)$), calculated for randomly oriented spheroids, are linearly related to absorbance; therefore, only the relative variations are significant. Raman spectra were recorded with a Jobin Ivon Ramanor U 1000 double monochromatic spectrometer using the 5145 Å Ar⁺ exciting line.

Theoretical Considerations

Rutile crystals belong to the symmetry group D_{4h}^{14} with two formula units per unit cell. Factor group analysis at $k = 0$ gives the following modes after subtracting the acoustic ones:

$$T = A_{1g}(R) + A_{2g} + A_{2u}(IR) + B_{1g}(R) \\ + B_{2g}(R) + 2B_{1u} + E_g(R) + 3E_u(IR)$$

Thus, the centrosymmetric group gives four vibrations ($A_{2u} + 3E_u$) infrared active and four vibrations ($A_{1g} + B_{1g} + A_{2g} + E_g$) Raman active. In the Raman modes only the oxygen atoms are allowed to move during the vibrations but in the infrared active vibrations titanium and oxygen ions are moving.

The infrared lattice vibrations of rutile have been studied by several authors (17, 18). The optical parameters (Table I) were obtained by analysis of single crystal reflection data (17) except for the A_{2u} mode which was taken from neutron scattering measurements (19).

The Raman spectrum of single-crystal ru-

tile has been also studied (20, 21) and the symmetry of the modes is given in Table I. It can be seen that two extra modes to those theoretically predicted were found at 235 and 320–360 cm⁻¹. Either disorder effects (22) or second-order scattering (23) has been claimed to explain the extra modes which are clearly observed also on powdered samples (23).

The analysis of the infrared powder spectra of rutile was carried out by using the TADC which has been described in full elsewhere (7) and only some important features will be given here. Three variables determine the infrared powder spectrum in this theory: (1) the dielectric constant of the matrix (ϵ_m) in which the material is diluted, (2) the shape of the microcrystals (g) and (3) the state of aggregation (f) of the particles. The effect of the matrix will not be considered since we have used KBr in all the experiments. The particle shape is assimilated in this theory to a revolution ellipsoid through a shape factor (g), and it is assumed that the axis of revolution is coincident with the crystallographic c axis of rutile. The shape factor associated with the c axis is called g_1 and tends toward 1 for plate-like morphologies and toward 0 for cylinder-like morphologies being 0.33 for spheres. Finally, the state of aggregation is defined through a filling factor (f) whose value ranges from 0 to 1. The f is the volume fraction occupied by the particles in the composite.

It should be noted that infrared spectra calculations carried out for rutile show that similar results are obtained for aggregated spheres and oblate spheroids. Consequently, the aid of electron microscopy is necessary to distinguish between both situations (8, 24).

Results and Discussion

Infrared Spectra

The infrared powder spectrum of the monodispersed powder obtained by the

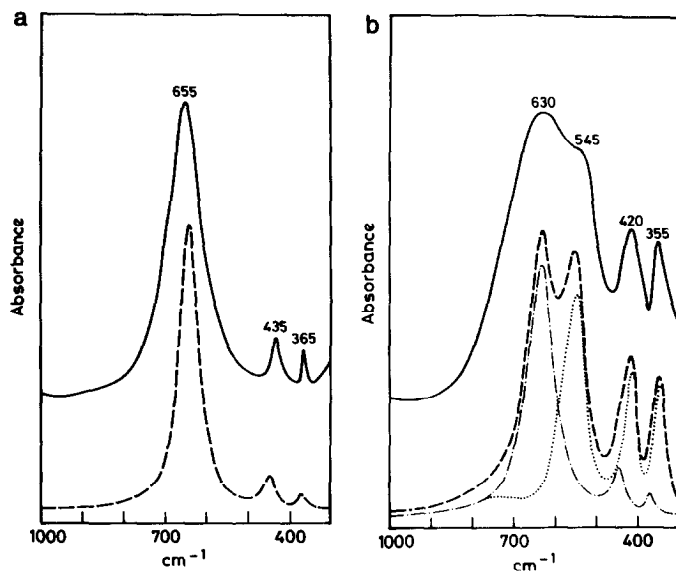


FIG. 3. Infrared spectra of rutile powders: (a) (—) Synthesized by the aerosol technique (Fig. 1a); (---) calculated for low aggregated spheres ($g_1 = 0.333, f = 0.1$). (b) (—) Synthesized by hydrolysis in alcoholic solution (Fig. 2a); (---) calculated with a mixture of spheres ($g_1 = 0.333, f = 0.2$) and oblate spheroids ($g_1 = 0.74, f = 0.2$).

aerosol technique is shown in Fig. 3a. This spectrum can be fairly well reproduced by the TADC based on spheres with very little aggregation ($f < 0.1$). The quality of the fit obtained confirms the applicability of the TADC to materials of such a high dielectric constant. The main difference between the experimental and calculated spectrum is the band broadening which is greater in the former. This difference can, at least partially, be explained by heterogeneous clustering of the particles in the matrix (4). It is interesting to note that the intense absorption at 655 cm^{-1} is actually the contribution of two modes with different symmetry (A_{2u}, ω_t at 172 cm^{-1} ; E_u, ω_t at 500 cm^{-1}).

Powders composed of spherical particles of nonuniform size such as that shown in Fig. 1b gave almost identical infrared spectrum (data not shown) to that of the monodispersed ones, indicating that particle size does not influence the infrared spectrum. This is in complete agreement with the the-

ory of absorption and scattering of radiation by small particles (25), since for particle sizes smaller than the radiation wavelength ($\sim 0 \mu\text{m}$) the infrared spectrum should be independent of the particle size. For greater particles sizes, nonhomogeneous polarization will cause the infrared spectrum of a powder to vary with the size of the particles. However, for these particle sizes comparison between experiment and theory is difficult due to the contribution of scattering over the absorption mechanism which prevents obtaining a good-quality experimental spectra. This is why most spectroscopists grind their samples to particle sizes less than about $2 \mu\text{m}$.

A completely different infrared spectrum was recorded for the monodispersed powder obtained by hydrolysis of titanium ethoxide in ethanol solution (Fig. 3b). According to the observations of the particles under the electron microscope (Fig. 2a), the infrared powder spectrum can be described

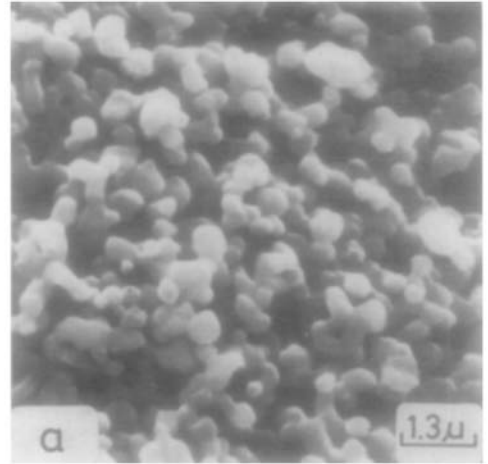
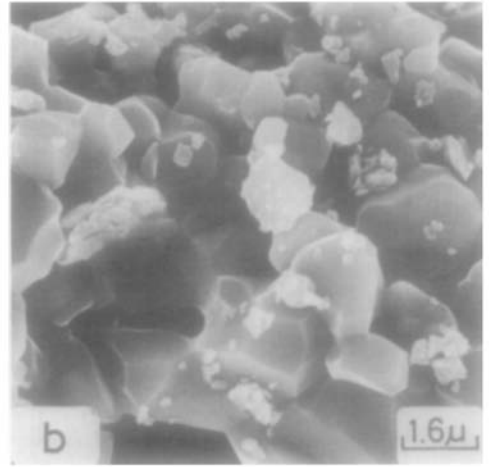
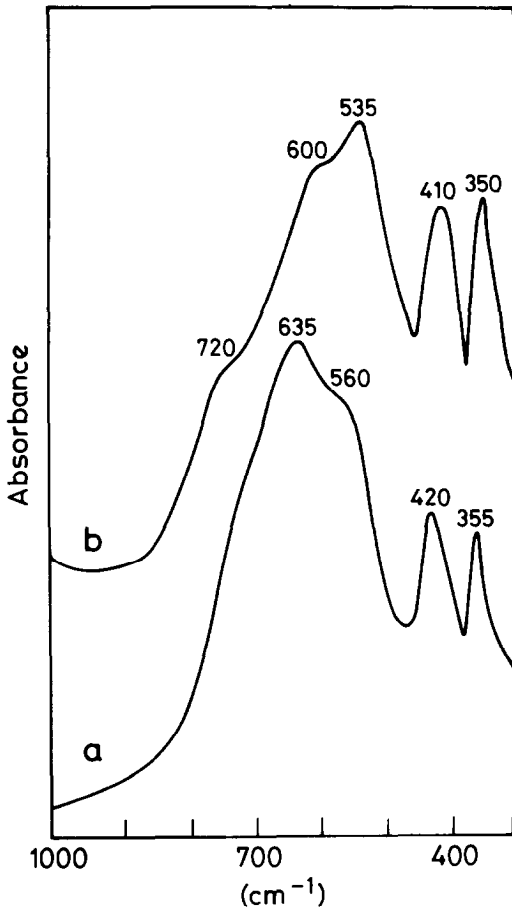


FIG. 4. Evolution with temperature of the monodisperse TiO₂ spherical sample obtained by the aerosol technique: (a) 1000°C, 4 hr; (b) 1300°C, 4 hr.

as a mixture of spheres and oblate spheroids coming from sintered spheres. Therefore, the absorption maxima at 630 and 545 cm^{-1} correspond to two different morphologies illustrating the usefulness of the infrared spectroscopy for the characterization of powders. It should be noted that the absorption band at 545 cm^{-1} can also be interpreted as being caused by spheres with high states of aggregation ($f = 0.65$) as it has been previously suggested (8).

Further support to the above interpretation can be obtained from the temperature evolution of the monodispersed powder synthesized by the aerosol technique. For this material, sintering starts at about 1000°C as observed by scanning electron microscopy (Fig. 4a). The spherical particles appear now more aggregated and some of them are clearly sintered giving an infrared spectrum (Fig. 4a) very similar to that of Fig. 3b. Thus, the shoulder at ~ 560

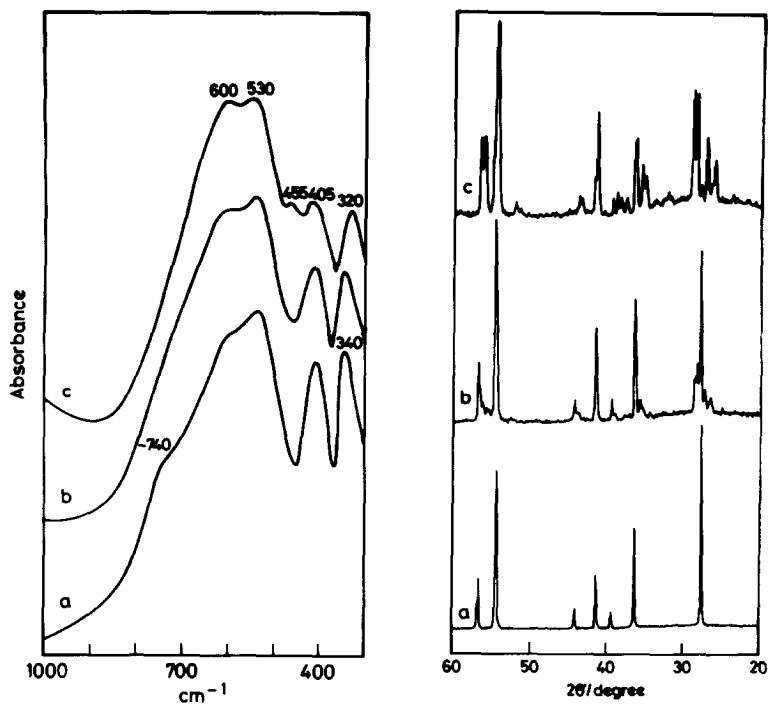


FIG. 5. Infrared spectra and X-ray diffraction patterns of high-temperature (1200°C) rutile powder (a) and its evolution at increased degrees of reduction (b and c).

cm^{-1} reflects the presence of the sintered spheres. The effect is still more evident as the process continues. In fact, at 1300°C (Fig. 4b) the band characteristic of the sintered material appears now at 535 cm^{-1} . This absorption band along with the shoulder at about 720 cm^{-1} are characteristics of plate-like morphologies. The band at $\sim 600\text{ cm}^{-1}$ corresponds to morphologies close to spheres and is due to the less reactive material (Fig. 4b). Finally, it must be noticed that the infrared spectrum of Fig. 4b, which is the most commonly published infrared powder spectrum of rutile, actually corresponds to that of a heterogeneous material.

The effect of nonstoichiometry was studied in a rutile sample heated at high temperature to ensure the lack of variability in particle shape during the reduction experi-

ments. The infrared spectra of the original sample and after several reduction treatments are shown in Fig. 5 along with the X-ray diffraction patterns of the samples. It is clear from the figure that stoichiometry variations do not have any important effect on the infrared spectrum of rutile. Only at very high reduction rates a new absorption band at 455 cm^{-1} and a shift of the band at 340 cm^{-1} to lower values were observed (Fig. 5c). However, under these conditions several Magneli-type phases ($\text{Ti}_n\text{O}_{2n-1}$, $4 \leq n \leq 9$) and the broad nonstoichiometric phase TiO_x ($0.70 \leq x \leq 1.30$) were present, as observed in the X-ray diffraction patterns (Figs. 5b and 5c). This last type of phase must be responsible for the 455 cm^{-1} absorption band since the Magneli phases ($\text{Ti}_n\text{O}_{2n-1}$) are built up of slabs of rutile-type structure. It can be concluded that nonstoi-

chiometric effects cannot be observed by infrared spectroscopy in currently prepared rutile samples.

Raman Spectra

Raman spectra from polycrystalline materials have been shown to present size and shape effects for samples whose vibrational modes are both infrared and Raman active, i.e., modes with translational character (13). The first unambiguous experimental observation on the particle size and shape effects in Raman scattering was recently published by Hayashi and Kanamori (10) in GaP microcrystals. As theoretically predicted, a new band was observed when the microcrystals were about one order of magnitude smaller than the wavelength of the incident laser radiation ($\sim 0.5 \mu\text{m}$). In addition, when the crystallite size decreases from 500 to 100 Å, surface effects become more and more important due to the increase in the surface to volume ratio. In fact, for very small microcrystals, a completely amorphous-like spectra was observed (10).

Since rutile structure belongs to a centrosymmetric group (D_{4h}^{14}), only surface effects should be observed. Consequently, all the above studied samples (crystallite size ~ 3000 Å) gave identical Raman spectrum (Fig. 6d), which were also identical to that reported in the literature (11, 23). This spectrum can be fully interpreted based on the single crystal spectrum (20). Thus, the Raman bands in Fig. 6, at 147, 446 and 610 cm^{-1} , correspond to the B_{1g} , E_g , and A_{1g} modes, respectively. The B_{2g} Raman active mode at 826 cm^{-1} could not be recorded due to its weak intensity. The broad Raman band at 235 cm^{-1} is also present in the single crystal Raman spectra and either second-order scattering or disorder effects have been suggested to explain its origin (20, 22).

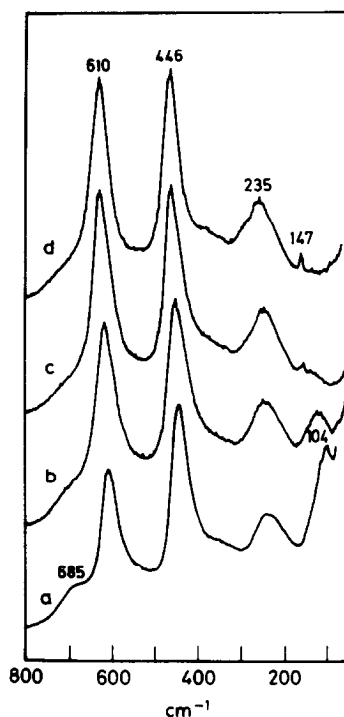


FIG. 6. Raman spectra of TiO_2 (rutile) powders obtained by hydrolysis of TiCl_3 at 98°C. (a) Initial sample; (b) heated at 200°C, 8 hr; (c) heated at 400°C, 8 hr; (d) heated at 1000°C, 8 hr.

For very small samples (~ 400 Å) new scattering bands were detected at about 685 and 104 cm^{-1} (Fig. 6a). Some kind of activation mechanism, based on the relaxation of the selection rules, could be postulated to explain the above bands. Thus, the band at 685 cm^{-1} could be assigned to the optically forbidden A_{2g} transition, and the band at 104 cm^{-1} could be attributed either to an A_{2u} acoustic vibration or to the B_{1u} optic mode. However, at the present, there is no appropriate explanation for these bands other than a manifestation of surface effects. Therefore, the new Raman bands seem to come from the surface layers of the microcrystals. In fact, these bands decrease in intensity as the particle size increases (or decreases the surface) on sinter-

ing (Fig. 6b), disappearing for particle sizes of about 600 Å (Fig. 6c).

Nonstoichiometric effects on Raman scattering spectra of rutile could not be studied due to difficulties in obtaining the Raman spectra of the reduced samples.

Acknowledgment

We thank Dr. González Carreño for the TiO₂ reduction experiments.

References

1. L. GENZEL AND T. P. MARTIN, *Surf. Sci.* **34**, 33 (1973).
2. S. HAYASHI, N. NAKAMORI, AND H. KANAMORI, *J. Opt. Soc. Japan* **46**, 176 (1979).
3. S. HAYASHI, J. HIRONO, H. KANAMORI, AND R. RUPPIN, *J. Phys. Soc. Japan* **46**, 1602 (1979).
4. C. J. SERNA, M. OCAÑA, AND J. E. IGLESIAS, *J. Phys. C* **20**, 473 (1987).
5. J. T. LUXON AND R. SUMMITT, *J. Chem. Phys.* **50**, 1366 (1969).
6. C. J. SERNA, J. L. RENDON, AND J. E. IGLESIAS, *Spectrochim. Acta Part A* **38**, 797 (1982).
7. M. OCAÑA, V. FORNÉS, J. V. GARCÍA RAMOS, AND C. J. SERNA, *Phys. Chem. Miner.* **14**, 117 (1987).
8. M. OCAÑA, V. FORNES, AND C. J. SERNA, "Processing Advanced Ceramics," p. 38, Soc. Esp. Ceram. Vid. Araganda del Rey, Madrid (1986).
9. S. HAYASHI, M. ITO, AND K. KANAMORI, *Solid State Commun.* **44**, 75 (1982).
10. S. HAYASHI AND K. KANAMORI, *Phys. Rev. B* **26**, 7079 (1982).
11. S. M. VOVK, M. YA. TSENKER, YA. S. BOBOVICH, AND L. M. SHARYGIN, *Opt. Spectrosc.* **55**, 476 (1983).
12. K. ISHIKAWA, N. FUJIMA, AND H. KOMURA, *J. Appl. Phys.* **57**, 973 (1985).
13. T. P. MARTIN AND L. GENZEL, *Phys. Rev. B* **8**, 1630 (1973).
14. M. VISCA AND E. MATIJEVIC, *J. Coll. Inter. Sci.* **68**, 308 (1979).
15. E. A. BARRINGER AND H. K. BOWEN, *J. Amer. Ceram. Soc.* **65**, C-199 (1982).
16. J. H. JEAN AND T. A. RING, "Proceedings, 38th Novel Ceram. Fabric. Process and its Appl.," p. 11, The Institute of Ceramic, University of Cambridge (1986).
17. W. G. SPITZER, R. C. MILLER, D. A. KLEINMAN, AND L. E. HOWORTH, *Phys. Rev.* **126**, 1710 (1962).
18. F. GERVAIS AND B. PIRIOU, *Phys. Rev. B* **10**, 1642 (1974).
19. J. G. TRAYLOR, H. G. SMITH, R. M. NICKLOW, AND M. K. WILKINSON, *Phys. Rev. B* **3**, 3457 (1971).
20. S. P. S. PORTO, P. A. FLEURY, AND T. C. DAMEN, *Phys. Rev.* **154**, 522 (1967).
21. G. A. SAMARA AND P. S. PEERCY, *Phys. Rev. B* **7**, 1131 (1973).
22. Y. HARA AND M. NICOL, *Phys. Status Solidi B* **94**, 317 (1979).
23. U. BALACHANDRAN AND N. G. EROR, *J. Solid. State Chem.* **42**, 276 (1982).
24. To be published.
25. H. C. VAN DE HULST, "Absorption and Scattering of Light by Small Particles," Wiley, New York (1957).